

Formation of double- Λ hypernuclei at PANDA

T. Gaitanos, A.B. Larionov*, H. Lenske, U. Mosel

Institut für Theoretische Physik, Universität Giessen, D-35392, Giessen, Germany

**Also at: Russian Research Center, Kurchatov Institute, 123182 Moskow, Russia*

email: Theodoros.Gaitanos@theo.physik.uni-giessen.de

Abstract

We study the formation of single- and double- Λ hypernuclei in antiproton-induced reactions relevant for the forthcoming PANDA experiment at FAIR. We use the Giessen Boltzmann-Uehling-Uhlenbeck (GiBUU) transport model with relativistic mean-fields for the description of non-equilibrium dynamics and the statistical multifragmentation model (SMM) for fragment formation. This combined approach describes the dynamical properties of strangeness and fragments in low energy \bar{p} -induced reactions fairly well. We then focus on the formation of double- Λ hypernuclei in high energy \bar{p} -nucleus collisions on a primary target including the complementary Ξ -induced reactions to a secondary one, as proposed by the PANDA Collaboration. Our results show that a copious production of double- Λ hyperfragments is possible at PANDA. In particular, we provide first theoretical estimations on the double- Λ production cross section, which strongly rises with decreasing energy of the secondary Ξ -beam.

Key words: BUU transport equation, Giessen-BUU, statistical multifragmentation model, antiproton-induced reactions, hypernuclei, PANDA experiment.

PACS numbers: **25.75.-q**, **21.65.+f**, 21.30.Fe, 25.75.Dw.

1 Introduction

The investigation of hypernuclei is directly related to various fundamental aspects of nuclear and hadron physics [1,2]. Of extreme interest are still incompletely known hyperon-nucleon and hyperon-hyperon interactions. The knowledge of these interactions is crucial for a better understanding of the strangeness sector of the hadronic equation of state, in particular, beyond ground state baryon density. For instance, compact astrophysical objects such as neutron stars might be strongly affected by the presence of hypermatter due to a considerable softening of the hadronic equation of state at very

high baryon densities [3–5], which, however, seems to be in contrast with the recently observed neutron star of about two solar masses [6]. Hypernuclear structure provides information around saturation density only, while the production of hypermatter in nuclear reactions induced by heavy ions and by antibaryons covers a broader region in baryon density, isospin asymmetry and single-particle energy [7–10]. Nuclear reactions further can be useful for the formation of exotic hypernuclei and help to understand the limits of the nuclear chart also into the strangeness sector [11]. Furthermore, the investigation of hypernuclei is important for spectroscopy of conventional nuclei [12–14], since single hyperons bound in finite nuclei do not experience the Pauli blocking and thus serve as probes for many-body dynamics.

The hypernucleus is a bound nucleus with one or more nucleons replaced by Λ -hyperons. So far only single- Λ (or $S = -1$ single-strange) and double- Λ (or $S = -2$ double-strange) hypernuclei have been found experimentally. In the first case the physical properties of the hyperon-nucleon interaction can be studied, while in double- Λ hypernuclei also the hyperon-hyperon interaction is accessible.

Experimental information on single- Λ hypernuclei is conventionally provided by spectroscopy using pion or kaon beams, by high energy protons, and by electroproduction [15,16]. In these cases the structure of rather cold hypernuclei at ground state density is explored. In reactions induced by intermediate energy heavy-ion beams, however, a quite different scenario is encountered: hyperons are produced at densities higher than saturation, and then can be captured by nuclear fragments. Therefore, in such reactions one might explore indirectly the high density behaviour of the hyperon-nucleon interaction. The production of single- Λ hypernuclei in reactions between heavy nuclei was first theoretically proposed by Kerman and Weiss [17]. Complementary studies then followed by several groups [18–20]. Very recently experiments at JLAB on hypernuclear spectroscopy have been started [8]. Recent observations on hypernuclei and antihypernuclei in relativistic heavy-ion collisions have been reported recently by the STAR Collaboration [21] (see also for an experimental overview Ref. [22]). Furthermore, the HypHI and FOPI Collaborations [23–25] at GSI have performed heavy-ion experiments where the experimental analysis on hypernuclei are still under progress. Also recent theoretical investigations have been started [26].

The formation of double- Λ hypernuclei is in the focus of strangeness-nuclear physics since the experimental discovery of the ${}^{10}_{\Lambda\Lambda}\text{Be}$ [27] and ${}^6_{\Lambda\Lambda}\text{He}$ [28] hypernuclei in the 60's by measuring their double pion decay (see Refs. [10,29] for the present experimental status of $\Lambda\Lambda$ -hypernuclei). For this purpose the copious production of rather slow Ξ -hyperons is necessary. One of the key projects in the new FAIR facility is the experimental investigation of double-strange hypernuclei by the PANDA Collaboration [30–33], which is the main

subject of this paper. Here one intends to form hypernuclei by reactions induced by antiprotons (\bar{p}) at beam momenta around 3 GeV/c, i.e., close to the $\Xi\bar{\Xi}$ production threshold ($P_{\text{lab}}^{\text{thr}} = 2.62$ GeV/c). In contrast to heavy-ion collisions and proton-induced reactions, where strangeness production proceeds mainly through meson rescattering and resonance decay, here the main production mechanism for hypernuclei arises from $\bar{p}p$ - and $\bar{p}n$ -annihilation. This channel has very high cross section at PANDA energies, i.e., $\sigma_{\bar{p}p} \simeq (60 - 80)$ mb, which is almost a factor of 2 higher than the corresponding pp cross section [34]. According to the PANDA proposals, double-strange hypernuclei are expected to be produced through the capture of primary cascade particles (Ξ) into secondary targets, which then are converted inside a nuclear fragment into two Λ hyperons.

Recently we have studied the formation of S=-1 single-strange hypernuclei in heavy-ion collisions and high energy proton-induced reactions [26]. Our theoretical estimates on the production probability of strangeness carrying nuclei seem to be compatible with the HypHI experiment [35] and are also close to other theoretical analyses [20]. Here we extend our previous investigations to the formation of double-strange hypernuclei in antiproton induced reactions at energies close to those of the proposed PANDA experiment [31] at FAIR. The theoretical treatment is based on a relativistic kinetic theory in the framework of the GiBUU transport model [36] supplemented by a statistical model of fragment formation [37]. The theoretical background is presented in Section 2. Detailed results on antiproton-induced reactions are then presented and discussed in Section 3. Conclusions and final remarks close this work in Section 4.

2 Transport theoretical framework

The fast non-equilibrium stage of hadron-nucleus reactions is described by the GiBUU transport model. GiBUU consists of a common transport theoretical framework for various reaction types, e.g., heavy-ion collisions, photon-, electron-, neutrino- and hadron-induced reactions. For a detailed description see [36]. Here we apply it to antiproton-induced reactions at PANDA energies and to reactions induced by low-energetic Ξ -hyperons.

The GiBUU model is based on a covariant extension of the semiclassical kinetic theory [38,39], the relativistic Boltzmann-Uehling-Uhlenbeck equation, which reads

$$\left[k^{*\mu} \partial_{\mu}^x + (k_{\nu}^* F^{\mu\nu} + m^* \partial_x^{\mu} m^*) \partial_{\mu}^{k^*} \right] f(x, k^*) = \mathcal{I}_{coll} \quad . \quad (1)$$

Eq. (1) describes the dynamical evolution of the one-body phase-space distribution function $f(x, k^*)$ for the hadrons under the influence of a hadronic mean-field (l.h.s. of Eq. (1)) and binary collisions. In the spirit of the relativistic mean-field (RMF) approximation of Quantumhadrodynamics the kinetic equation is formulated in terms of kinetic 4-momenta $k^{*\mu} = k^\mu - \Sigma^\mu$ and effective (Dirac) masses $m^* = M - \Sigma_s$. The self-energy is given by its Lorentz-vector (Σ^μ) and Lorentz-scalar (Σ_s) components

$$\begin{aligned}\Sigma^\mu &= g_\omega \omega^\mu + \tau_3 g_\rho \rho_3^\mu \\ \Sigma_s &= g_\sigma \sigma \quad ,\end{aligned}\tag{2}$$

with the isoscalar, scalar σ , the isoscalar, vector ω^μ meson fields. ρ_3^μ is the third isospin-component of the isovector, vector meson field, and $\tau_3 = \pm 1$ for protons and neutrons, respectively. The self-energies describe the interaction between nucleons inside infinite nuclear matter, where the classical meson fields obey the standard Lagrangian equations of motion [40]. The meson-nucleon coupling constants g_i ($i = \sigma, \omega, \rho$) and also the additional parameters of the non-linear self-interactions of the σ meson (not shown here) are taken from the widely used NL parametrizations [41].

Since we will study antiproton-nucleus reactions, we need the antinucleon-meson vertices, too. In principle, the description of the in-medium antinucleon interaction should be based on the properties of the strong interaction under G-parity transformation. G-parity transformation of the nucleon field, as in Eq. (2) is equivalent with a sign change of only the isoscalar Lorentz-vector component of the baryon self-energy. However, the conventional RMF approach fails to describe empirical data on antiproton production in p -nucleus and nucleus-nucleus interactions by imposing only G-parity [42]. This problem has been related to a linear energy dependence of the proton-nucleus optical potential, which is not consistent with empirical data and results to a divergent linear behavior for the antinucleon-nucleus interactions. A way to overcome this issue has been recently proposed in [43–45], using non-linear derivative interactions. Indeed, not only the energy dependence of the real part of the in-medium antinucleon interaction turned out to be in agreement with available data [44]. Also the imaginary (dispersive) part of the in-medium antinucleon optical potential significantly contributes to the energy dependent in-medium antinucleon interaction, again in agreement with empirical studies [44]. For the description of complex nuclear dynamics such as heavy-ion collisions within transport theory a simpler approach for the RMF fields is applied here. The antinucleon-meson coupling constants are rescaled by a phenomenological parameter such, to reproduce experimental data in high energy antiproton-induced reactions [46].

Numerically, the collision term is treated in a parallel ensemble algorithm incorporating the standard parametrizations for the cross sections of various

binary processes [36]. Important for this work is the recent implementation in GiBUU [46,47] of $\bar{N}N$ -annihilation channels according to a statistical model of Pshenicknov et al. [48], including $\bar{K}KX$ mesonic final states. Furthermore, the following primary channels have been implemented recently (Y, N stand for hyperons and nucleons, respectively): $\bar{N}N \rightarrow \bar{Y}Y$, where the channel $\bar{N}N \rightarrow \bar{\Xi}\Xi$ is of particular interest. Their parametrizations are given in Refs. [47,49]. Secondary interactions involving hyperons contribute also to the production of hypernuclei. Among the various secondary processes, the channels $\bar{K}N \rightarrow \Xi K$ and $\Xi N \rightarrow \Lambda\Lambda$ are essential for hypernuclear formation. The cross section of the former binary collision is taken from [50–53], while the cross section for the latter process is taken from a parametrization to theoretical calculations [54].

The present implementation of the GiBUU model turned out to work well for strangeness production at PANDA energies, as shown in Ref. [47]. However, for the description of single- and double- Λ hypernuclei not only the yields and spectra of produced strange particles should be in agreement with experiment, but also the fragmentation of the residual target source. As a well-known problem, Boltzmann-like transport equations do not provide information of the dynamical evolution of physical fluctuations. Thus, one has to model fragment formation by coalescence or using complementary statistical models. Previously, we have applied the statistical multifragmentation model (SMM) from Botvina et al. [37] to spectator fragmentation and to the decay of residual nuclei in reactions induced by protons and heavy ions [26,55] for the formation of nuclear fragments. It turned out that the hybrid GiBUU+SMM approach reproduces the data on fragmentation with high accuracy. The combination between the pre-equilibrium dynamics (GiBUU) and the fragmentation stage (SMM) in hadron-induced reactions consists of the following steps: at first, we calculate the average mass $\langle A \rangle$, charge $\langle Z \rangle$ and excitation energy E^* of the bound system (residual source) as a function of time, where bound particles are selected by a simple density cut. The excitation energy is obtained event-by-event from energy balance. When the average properties of the residual bound system do not experience any time dependencies, we stop the simulation and switch to the SMM model. We also determine the anisotropy ratio at the central shell of the residual source. It gives complementary information on the degree of local equilibration of the system, which is required by the SMM model.

Numerically the GiBUU equations are solved within the test particle method, where the phase-space distribution function is discretized by so-called test particles [56]. One then solves the relativistic Hamiltonian equations of motion for the test particles, while the collision term is simulated by standard Monte Carlo prescriptions. In such computational simulations spurious numerical noise is unavoidable. Important for the present study is a very good stability of the ground state nucleus, which is not obvious within the test particle formalism. A very good nuclear ground state stability is also required,

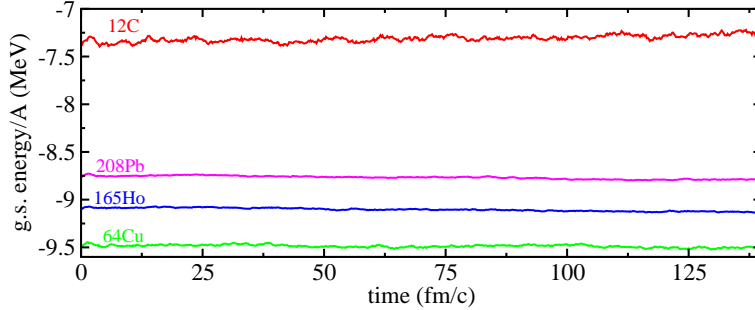


Fig. 1. Ground state (g.s.) energy per nucleon (subtracting the nucleon mass) as function of time for different targets, as indicated. The calculations were performed in the Vlasov mode, i.e., without including binary collisions.

in order to avoid spurious particle emission and non-conservation of energy. This issue is important when determining the excitation energy of a residual system. As described in detail in Ref. [57], we use the same energy density functional to extract the ground state density profiles needed for the initialization and to propagate then the system. The results of this improved initialization prescription are shown in Fig. 1. As one can see, the ground state energy is almost perfectly stable in time. In particular, for the heavier systems energy conservation is perfect. More details on this study can be found in Ref. [57]. We therefore expect that the excitation energy in reactions with these nuclear targets is extracted in a reliable way by reducing spurious contributions as much as possible.

3 Results

With the improved initial target configurations reactions with antiproton beams have been performed, first, at low incident energies of 1.22 GeV, where data on excitation energy and fragment yields are available [58], and then at higher energies around the $\Xi\bar{\Xi}$ production threshold ($P_{\text{lab}} = 2.62$ GeV/c beam momentum or $E_{\text{lab}} = 1.84$ GeV incident energy). In the latter case complementary reactions with Ξ -beams have also performed. The properties of the residual source have been extracted by counting only bound particles, as explained in the previous section. After freeze-out we apply the SMM model [37] to simulate the decay of the excited residual source. These calculations are denoted as GiBUU+SMM.

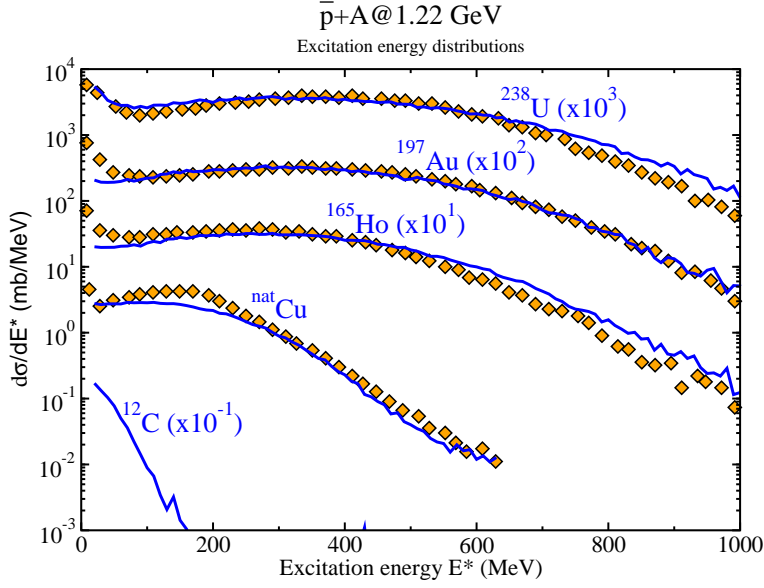


Fig. 2. Inclusive excitation energy distributions for \bar{p} -induced reactions at an incident energy of 1.22 GeV on various targets, as indicated. The GiBUU+SMM calculations (solid curves) are compared to available experimental data (filled symbols), taken from [58]. The curves are multiplied by successive powers of 10 starting from $^{\text{nat}}\text{Cu}$.

3.1 Fragment production in antiproton-induced reactions

Fig. 2 shows the theoretical results for the inclusive excitation energy distributions in comparison with experimental data. The shape and also the absolute values of the experimental distributions are reproduced fairly well by the transport calculations. The application of the SMM code after freeze-out provides single nucleons and fragments. Fig. 3 shows the particle yields as the result of the combined GiBUU+SMM approach. The comparison with the experimental data for various types of fragments - in shape and absolute values - is very good, except for the very light systems. Note that the cases $Z = 1$ and charged particles include also emitted protons from the pre-equilibrium GiBUU stage.

Similar complementary fragmentation studies have been performed for proton-induced reactions and for spectator fragmentation in heavy-ion collisions [55], again with a satisfactory description of fragment yields and their spectra. In the following we will explore also the formation of hypernuclei. Therefore, apart from the requirement of a correct description of the fragmentation, a reliable dynamical description of particle production is also very important, in particular, for resonances as well as for pions, kaons and hyperons. Particle production in antiproton-induced reactions has been found to work well, as discussed in detail in Refs. [46,47]. At this level of investigation we conclude that the combination of the GiBUU transport model together with the SMM

$\bar{p} + A @ 1.22 \text{ GeV}$

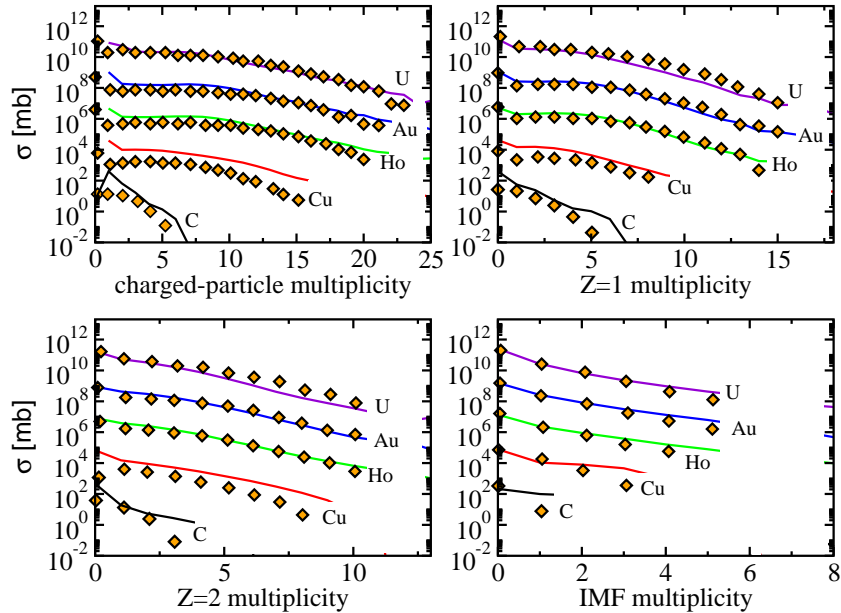


Fig. 3. Inclusive fragment multiplicity distributions for \bar{p} -induced reactions at an incident energy of 1.22 GeV on different targets, as indicated. Upper panel on the left: charged-particles, upper panel on the right: protons and $Z = 1$ -fragments, lower panel on the left: $Z = 2$ -fragments, and lower panel on the right: intermediate mass fragments (IMF). The GiBUU+SMM calculations (solid curves) are compared with the data [58] (filled symbols). The curves are multiplied by successive powers of 10^2 starting from C .

approach represents a reliable method for the dynamical description of the entire process, starting from the pre-equilibrium dynamics up to the clusterization of the excited system.

3.2 Proton- versus antiproton-induced reactions

Reactions induced by protons [18] and heavy-ions [26] turned out to be a useful tool for studies on single- Λ hypernuclei. However, the formation of double-strange hyperfragments has not been investigated in detail, neither experimentally nor theoretically, so far. As proposed by the PANDA Collaboration, reactions with antiprotons are expected to be an ideal environment for the production of double- Λ hypernuclei [30–33]. At first, by looking at typical properties such as mass and charge numbers and excitation of the bound system, no differences are visible between proton- and antiproton-induced reactions. This is demonstrated in Fig. 4 in terms of the time evolution of these quantities at an incident energy of $E_{\text{lab}} = 5 \text{ GeV}$. In the p -induced reactions the protons penetrate deeply into the nucleus, and the energy transfer is caused by multiple rescattering with resonance production and absorption of mesons.

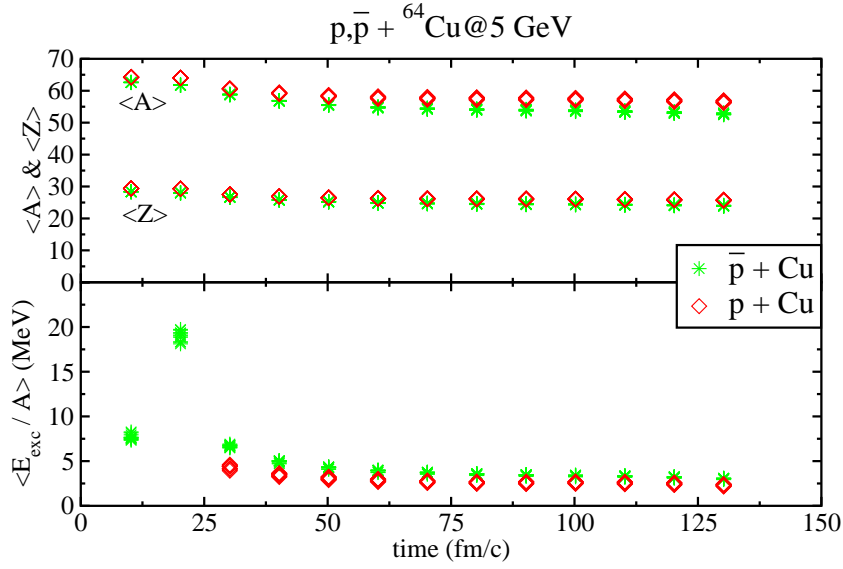


Fig. 4. Time evolution of the average mass $\langle A \rangle$, the average charge $\langle Z \rangle$ (upper panel, as indicated) and the average excitation energy per nucleon $\langle E_{\text{exc}}/A \rangle$ (lower panel), as the result of GiBUU calculations, for proton-induced (open diamonds) and antiproton-induced (filled stars) reactions at an incident energy of 5 GeV and impact parameter of $b=3.4$ fm. For the $p+\text{Cu}$ reaction the excitation energy at early times is $\simeq 40$ MeV/nucleon and not visible in the lower figure.

A quite different reaction scenario is found in antinucleon-induced reactions. The strong absorption confines interactions to a small layer at the nuclear surface. Hence, in the $\bar{p} + \text{Cu}$ case the antiprotons do not penetrate much into the nuclear interior, and annihilate mainly close to the nuclear surface. In a $\bar{p}N$ annihilation final states with many mesons are locally produced [59]. This creates a peak in the excitation energy at $t \sim 20$ fm/c, see Fig. 4, due to the excitation of the residual nucleus by annihilation mesons. Multiple meson-nucleon re-scattering is also possible in this case. Thus one expects a similar energy transfer as in the proton-nucleus case at long time scales, as also shown in Fig. 4.

The major difference between the proton-nucleus and antiproton-nucleus cases appears in the multiplicities of various produced particle species. While in the first case final channels with only few mesons (pions, kaons, antikaons) are mostly probable, the predominant channel in antiproton-nucleus collisions is the annihilation into many-body final states. Thus, not only mesons (mostly pions, and then kaons/antikaons), but also many-body final states with hyperons/antihyperons can be created in annihilation. This difference in the particle yields between proton- and antiproton induced reactions can be seen in Fig. 5. Most of the particle yields are enhanced by almost a factor of two in the \bar{p} -induced reactions, in particular the increase of the antikaon yield is remarkable. In fact, in the p -nucleus case antikaons can be formed only in 4-

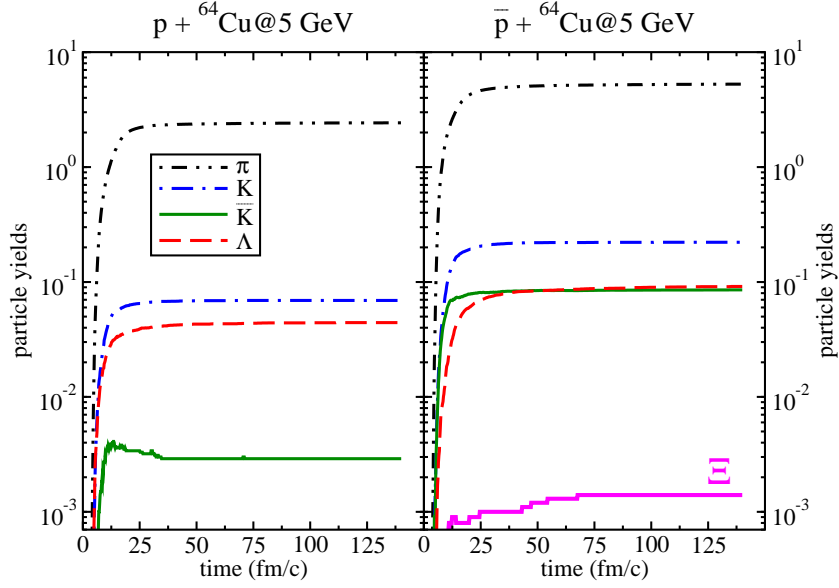


Fig. 5. GiBUU calculations for the yields of various particle species (as indicated) as function of time in proton-induced (left panel) and antiproton-induced (right panel) reactions at an incident energy of 5 GeV and impact parameter of $b=3.4$ fm. The cascade Ξ -particle, which is indicated inside the right panel, is produced only in antiproton-induced events.

body final states in the process $pN \rightarrow NNK\bar{K}$ which has a very low branching ratio. On the other hand, in the \bar{p} -case the production of $K\bar{K}$ -pairs in pure mesonic annihilation events is possible. Thus the \bar{K} -yield dramatically rises in antiproton-induced reactions. Another difference between the two reaction cases appears in the production of the cascade Ξ -particle, which appears only in antiproton-nucleus collisions. Its yield is extremely low because of the low production cross section for the primary process $\bar{p}p \rightarrow \Xi\bar{\Xi}$ [60]. Note that cascade particles can be produced in secondary processes involving antikaons, mostly in the process $\bar{K}N \rightarrow \Xi K$ [61].

3.3 Production of $S = -2$ hypernuclei in $\bar{p} + A$ -reactions

Our study shows that in antiproton-induced reactions a copious production of hyperons is possible, which enhances the probability for the production of hypernuclei, in particular, those with two captured Λ hyperons. A particular candidate for the formation of double-strange matter is expected to be the cascade particle. However, an answer on the question, whether the cascade particles give the major contribution to the formation of double-strange hypernuclei or not, depends on two issues. First, the Ξ particles have to be slow in order to be captured inside the residual system, otherwise the relativistic mean-field, in particular its Lorentz-vector component, is too repulsive and

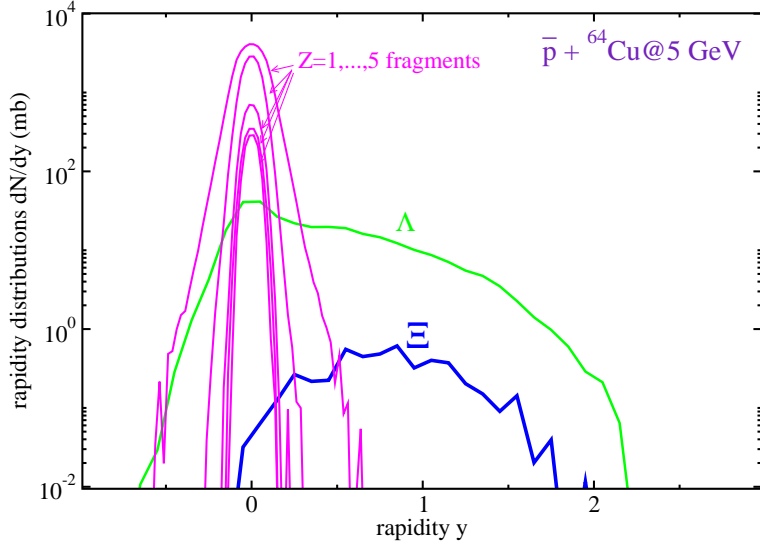


Fig. 6. GiBUU+SMM calculations for the rapidity distributions of fragments with charge $Z = 1, \dots, 5$ and hyperons with strangeness $S = -1$ (Λ) and $S = -2$ (Ξ), as indicated, for inclusive $\bar{p} + \text{Cu}@5$ GeV reactions.

the resulting effective potential too shallow for a capture into a bound state. Secondly, the cross section for the process $\Xi N \rightarrow \Lambda \Lambda$ must be high enough, and, at least, comparable with the corresponding elastic $\Xi N \rightarrow \Xi N$ and also quasi-elastic $\Xi N \rightarrow \Lambda \Sigma$ processes.

The PANDA Collaboration [30–32] has proposed an experiment consisting of two targets. The primary target serves for the production of the cascade particles through the interaction of the antiproton beam with the target nucleons. The emitted Ξ -particles will be decelerated by ionization energy loss in ordinary matter before their interaction with a secondary target. In this way one assumes that the slow moving Ξ -particles will be captured by the secondary target, and the formation of double-strange hypernuclei will occur after the conversion of the bound Ξ 's into two Λ -hyperons inside the secondary residual nucleus by the collision with a nucleon.

Before analyzing the scenario with the secondary target, i.e., performing GiBUU studies for Ξ -induced reactions, it is useful to investigate the strangeness dynamics, in particular the properties of the produced Ξ hyperons, from the antiproton interaction with a primary target. We have performed GiBUU+SMM calculations for inclusive \bar{p} -interactions with a ^{64}Cu target nucleus at an incident energy of $E_{\text{lab}} = 5$ GeV.

Fig. 6 shows the rapidity spectra of various fragments and single hadrons produced in $\bar{p} + \text{Cu}$ reactions at an incident energy of $E_{\text{lab}} = 5$ GeV. Various intermediate mass fragments (and also heavier residues not shown in this figure)

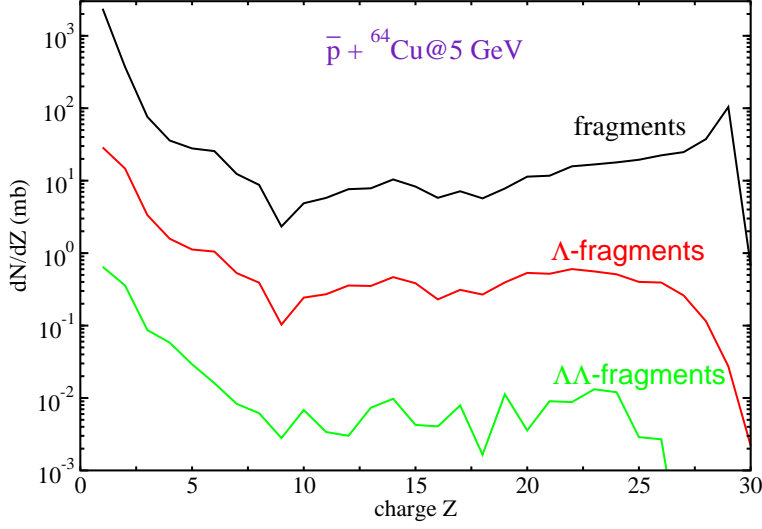


Fig. 7. GiBUU+SMM calculations for the charge distributions of nuclear fragments (upper curve), of single- Λ (middle curve) and double- Λ (lower curve) hyperfragments.

are produced close to the rest frame of the target. The rapidity distributions of various particles with strangeness are quite different. Hyperons with $S = -1$ (Λ particles) show a broad spectrum in rapidity, while particles with $S = -2$ (Ξ particles) are rather located at high rapidities. The difference between the rapidity spectra of hyperons with $S = -1$ and $S = -2$ arises from the different way how these particles are produced. As discussed above, Λ particles can be produced in various processes. Direct production in the annihilation channel $\bar{p}p \rightarrow \bar{\Lambda}\Lambda(M)$ in first collisions provides the high energy tail of the rapidity distribution. However, Λ particles undergo multiple secondary scattering with nucleons which redistributes their velocities. On the other hand, the channel $\bar{K}\Lambda \rightarrow \bar{\Xi}N$ gives the major contribution to Ξ production. Such type of a secondary process is possible only when the energy of the initial antikaon is high, because of the high threshold $\sqrt{s_{\text{thr}}} = M_{\Xi} + M_N = 2.253$ GeV requiring a minimal kinetic energy of $E_{\text{kin}} \simeq 2.13(1.7)$ GeV for the antikaon (Λ hyperon) in the cm-frame. Thus, the Ξ production is shifted to high rapidities. The produced cascade particles can leave the bound system, while most of the Λ hyperons are captured. In addition to collisions, the relativistic mean-field plays also an important role for the capture of hyperons, in particular, for the low energetic ones, as discussed in more detail in Ref. [47].

Fig. 7 shows the results for the charge distributions of nuclear fragments, single- Λ and also double- Λ hypernuclei, as indicated. The nuclear fragments show the typical distribution with the evaporation peak close to $Z \simeq Z_{\text{targ}}$, the fission hill around $Z \simeq Z_{\text{targ}}/2$ and the power-low ($Z^{-\tau}$) multifragmentation region at smaller Z ($2 < Z < 8$). The formation of hyperclusters arises mainly

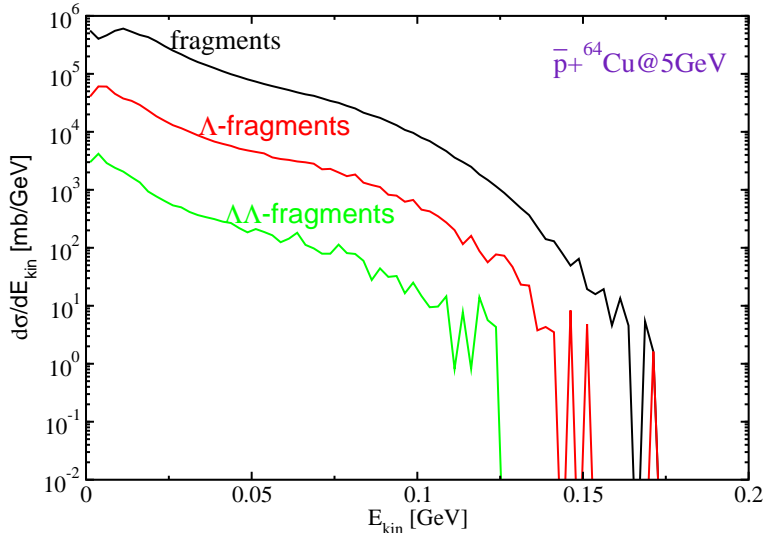


Fig. 8. Same as in the previous Fig. 7, but now for the kinetic energy spectra.

due to the momentum coalescence of the captured Λ -particles with the SMM-fragments. However, the yield of light double-strange hyperfragments is around three orders of magnitudes less relative to that of nuclear fragments. We note that the inclusion of the mean-field for the hyperons is important for the production of hypernuclei. Indeed, Λ -hyperons feels an attractive in-medium optical potential at low energies, which at saturation density is around -38 MeV. This attractive potential is also responsible for the binding mechanism of the slow-moving Λ -particles inside the residual target nucleus, as discussed in detail in Ref. [47].

Fig. 8 shows the kinetic energy distributions for nuclear fragments and hyperfragments with $S = -1$ and $S = -2$ strangeness content. Again the yield of double- Λ hypernuclei is very low, as already shown in the previous figure. Fig. 8 demonstrates that various particles are emitted from a thermalized residual source, since the slopes of various particle types are very similar.

3.4 Secondary hypernuclear formation by Ξ -beams

So far we have considered the properties of hypermatter in collisions between antiprotons with only the first target. As an intermediate result, a coalescence between fragments of the primary target with cascade particles occurs, however, with very low probability due to the high velocities of the produced cascade particles. In the considered example $\bar{p} + \text{Cu}@5$ GeV the maximum of the rapidity distribution (see again Fig. 6) of the Ξ -particles lies around $y \simeq 1$ corresponding to a kinetic energy (momentum) of $E_{\text{kin}} \simeq 0.7$ GeV ($p \simeq 1.54$

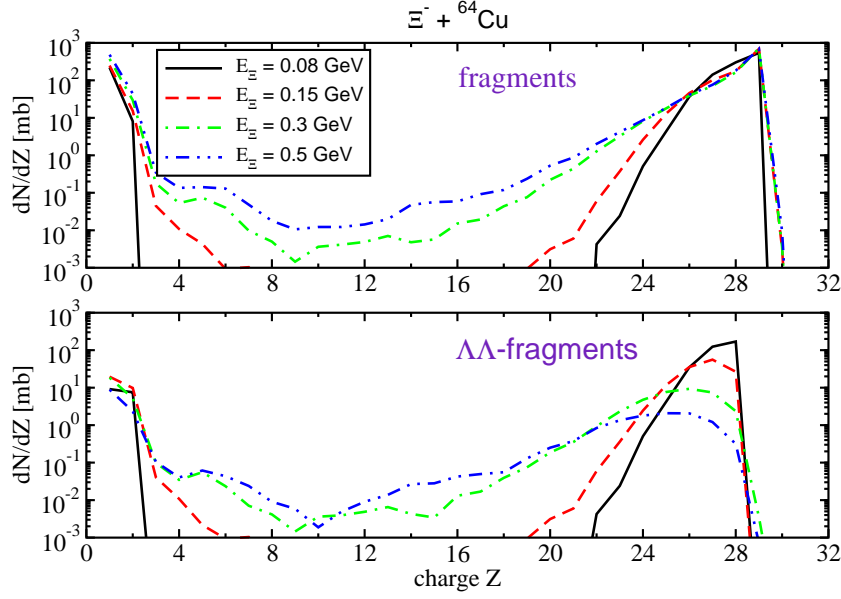


Fig. 9. GiBUU+SMM calculations for the charge distributions of nuclear fragments (upper panel) and double- Λ clusters (lower panel) for $\Xi^- + {}^{64}\text{Cu}$ reactions at various kinetic energies of the Ξ -beam in the laboratory frame, as indicated.

GeV/c).

In order to estimate the dynamical properties of the collisions with the secondary target, we have performed complementary transport calculations with Ξ^- -beams on the same target (${}^{64}\text{Cu}$) at incident kinetic energies of $E_{\text{lab}} = 0.08, 0.15, 0.3, 0.5$ GeV which correspond to the region just below the maximum value of the rapidity of the Ξ -particles. Fig. 9 shows the results for $\Xi^- + \text{Cu}$ -reactions at the beam energies as indicated. The nuclear fragment charge distributions reveal an U-shape typical for the quasi-fission and quasi-evaporation decay modes of medium heavy nuclei ($A \sim 60 - 100$) [37] at low excitation energies, in contrast to the multifragmentation pattern of Fig. 7. Another important difference with respect to the \bar{p} -induced reactions is that now each reaction event contains a Ξ particle, which collides with the bound nucleons producing two Λ particles and, therefore, leading to the production of $\Lambda\Lambda$ -hyperfragments with large probability. Thus, the distributions of the nuclear fragments and of the double- Λ hypermatter are very similar in the absolute values, as seen in Fig. 9. As a general trend, the production of double-strange hypernuclei decreases with increasing Ξ energy (see again lower panel in Fig. 9). In particular, the abundance of heavy hyperfragments reduces significantly as the beam energy rises. Since heavy residues mostly survive in peripheral events, the probability to form a $\Lambda\Lambda$ -hypernuclei obviously strongly decreases with increasing Ξ -beam momentum.

In total, it turns out that the double-strange hypernuclei yield produced in reactions between the Ξ -beam and the secondary target strongly decreases

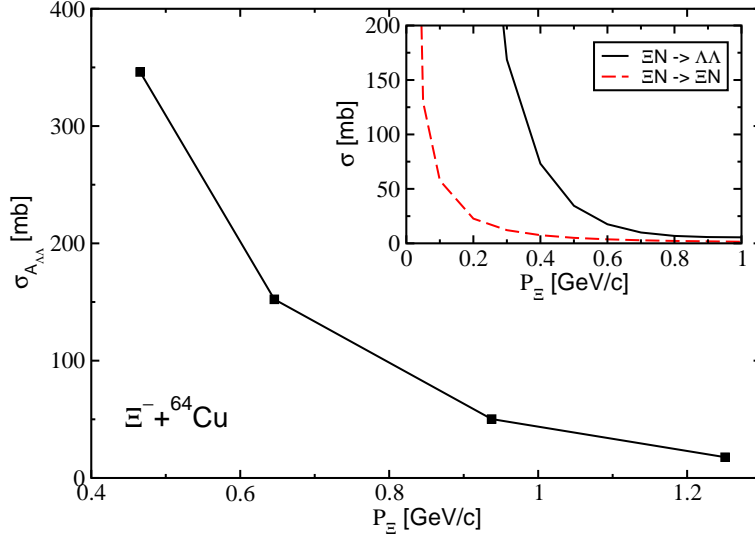


Fig. 10. (Main panel) Production cross section for double-strange hypermatter as function of the Ξ -beam momentum. The insert panel shows the elementary cross sections [54] for the indicated elementary channels.

with increasing beam energy (see Fig. 10). This is because of the quickly dropping $\Xi^- p \rightarrow \Lambda\Lambda$ elementary cross section as compared to the elastic one. This is shown in the inner panel in Fig. 10 for theoretical calculations according to the extended soft core model [54] for the elastic $\Xi N \rightarrow \Xi N$ and inelastic $\Xi N \rightarrow \Lambda\Lambda$ channels. Indeed, for momenta higher than 0.4 GeV/c the relevant inelastic channel strongly drops and becomes comparable with the elastic cross section. We conclude that in order to measure double-strange hypernuclei with very high cross section, the cascade particles produced in collisions between the antiproton beam with the primary target should have as low energy as possible. Indeed, in the PANDA experiment the emitted cascade particles are supposed to traverse a material for deceleration, before the collision with the secondary target system.

For the determination of the total production cross section of double-strange hypernuclei one needs the momentum distribution of the Ξ -particles emitted from the antiproton-reaction with the primary target. Fig. 11 shows this in the insert panel, again together with the double-strange hypernuclear cross section. As one can see from Fig. 11, the region around $P_{\Xi} \simeq 0.5 - 1.2$ GeV/c will contribute mostly to the total production cross section, for the considered $\bar{p} + ^{64}\text{Cu}@5$ GeV reaction. Thus, the effective value of the total double-strange hyperfragment cross section is estimated to be of the order of several mb, as the result of a momentum integration folding between $\sigma_{A_{\Lambda\Lambda}}(p_{\Xi})$ and $\frac{d\sigma}{dp_{\Xi}}$ and after consideration of attenuation of the Ξ hyperon due to its finite lifetime.

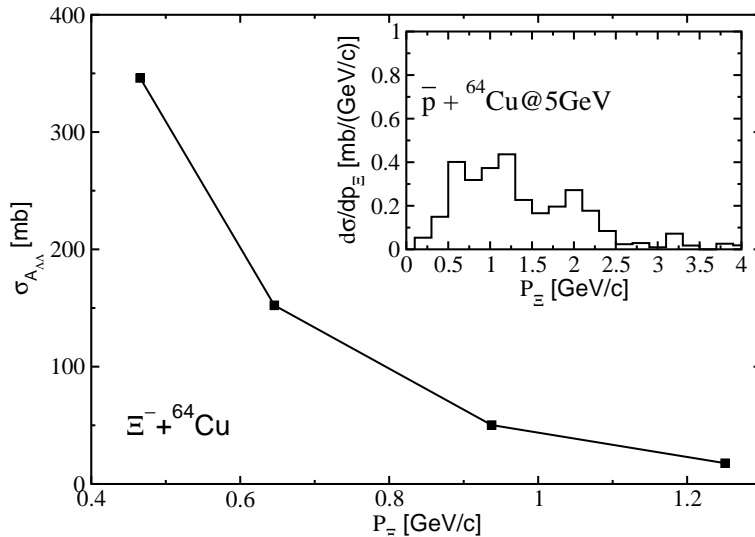


Fig. 11. (Main panel) Same as in Fig. 10. The insert panel shows now the Ξ -production cross section from \bar{p} -collisions on the first target, as indicated.

4 Conclusions and outlook

In summary, we have studied the formation of hypernuclei in reactions relevant for the PANDA project at the new FAIR facility. We have investigated hypernuclear production in two steps, as suggested in the proposal of the PANDA experiment, using the GiBUU transport theoretical framework for the description of the pre-equilibrium dynamics, and the SMM model for fragment formation. A supplementary momentum coalescence between hyperons and SMM-fragments has been adopted for the production of hyperfragments. For antinucleon-nucleon interactions an extension of the GiBUU approach was necessary by including more binary processes involving the scattering between nucleons and hyperons.

The combined GiBUU+SMM approach had earlier been shown to work well concerning the spectra and yields of produced strange particles and nuclear fragments in low energy antiproton-nucleus reactions. We have applied then the same model to antiproton induced reactions at higher energies. It was found that a simple coalescence between nuclear clusters and Λ -hyperons to single-strange hypernuclei is possible already in antiproton collisions with a first target. However, the formation of double-strange hypernuclei and the capture of double strange Ξ -particles occurs with very low probability, due to the high energies of the produced cascade hyperons. Thus, as suggested by the PANDA experiment, the Ξ particles have to be decelerated in order to be captured into a secondary target. This scenario is supported by the present transport simulations. The main mechanisms leading to the forma-

tion of double- Λ hypernuclei are the attractive mean-field and, in particular, the inelastic process $\Xi N \rightarrow \Lambda\Lambda$, whose cross section dramatically rises with decreasing Ξ energy.

At this level of investigation the predictive power of the theoretical calculations on hypernuclei is to some extent limited by incomplete knowledge on YN - and YY -interactions in free space and in nuclear matter. However, we are confident about our results by recalling that the underlying processes of strangeness production and fragmentation are well described, reproducing existing data very satisfactorily. We have estimated the production cross sections of double strange hypernuclei as function of the Ξ -hyperon energy by its capture with the secondary target. As an important result, double-strange hypernuclear production at PANDA is possible with high probability, if low energy cascade-particle beams will be used. We emphasize the relevance of our theoretical results for the future activities at FAIR.

Acknowledgments. We would like to thank A. Botvina for providing us the code for the Statistical Multifragmentation Model (SMM). This work is supported by BMBF contract GILENS 06, DFG contract Le439/9-1 and HIC for FAIR.

References

- [1] J. Haidenbauer, U. -G. Meissner, A. Nogga, H. Polinder, Lect. Notes Phys. **724** (2007) 113.
- [2] E. Friedmann, A. Gal, Phys. Rept. **452** (2007) 89.
- [3] N. K. Glendenning, New York, USA: Springer (1997) 390 p.
- [4] J. Schaffner-Bielich, Nucl. Phys. **A835** (2010) 279.
- [5] F. Hofmann, C. M. Keil, H. Lenske, Phys. Rev. **C64** (2001) 025804.
- [6] P. Demorest, T. Pennucci, S. Ransom, M. Roberts, J. Hessels, Nature **467** (2010) 1081.
- [7] T. R. Saito, S. Bianchin, O. Borodina, V. Bozkurt, B. Gokuzum, M. Kavatsyuk, E. Kim, S. Minami *et al.*, Nucl. Phys. **A835** (2010) 110.
- [8] O. Hashimoto, A. Chiba, D. Doi, Y. Fujii, T. Gogami, H. Kanda, M. Kaneta, D. Kawama *et al.*, Nucl. Phys. **A835** (2010) 121.
- [9] A. Sanchez Lorente, J. Pochodzalla, A. Botvina, Int. J. Mod. Phys. **E19** (2010) 2644.
- [10] J. Pochodzalla, Nucl. Phys. **A754** (2005) 430.
- [11] S. Aoki, S.Y. Bahk, S.H. Chung, H. Funahashi *et al.* (KEK E176 Collaboration), Nucl. Phys. **A828** (2009) 191.

- [12] E. Hiyama, M. Kamimura, Y. Yamamoto, T. Motoba, T. A. Rijken, Prog. Theor. Phys. Suppl. **185** (2010) 106.
- [13] E. Hiyama, M. Kamimura, Y. Yamamoto, T. Motoba, T. A. Rijken, Prog. Theor. Phys. Suppl. **185** (2010) 152.
- [14] A. S. Lorente, A. S. Botvina, J. Pochodzalla, Phys. Lett. **B697** (2011) 222.
- [15] A. M. Faessler *et al.*, Phys. Lett. **B46** (1973) 468;
R.E. Chrien *et al.*, Phys. Lett. **B89** (1979) 31;
M. Akei *et al.*, Nucl. Phys. **A534** (1991) 478;
F. Dohrmann *et al.*, Phys. Rev. Lett. **93** (2004) 242501.
- [16] O. Hashimoto, H. Tamura, Prog. Part. Nucl. Phys. **57** (2006) 564.
- [17] A.K. Kerman, M.S. Weiss, Phys. Rev. **C8** (1973) 408.
- [18] Z. Rudy *et al.*, Z. Phys. **A351** (1995) 217.
- [19] J. Aichelin, K. Werner, Phys. Lett. **B274** (1992) 260.
- [20] M. Wakai, Nucl. Phys. **A547** (1992) 89c.
- [21] STAR Collaboration, Science **328** (2010) 58.
- [22] J. Pochodzalla, Acta Phys. Polon. **B42** (2011) 833.
- [23] C. Rappold, T. R. Saito, S. Bianchin, O. Borodina *et al.*, Nucl. Instrum. Meth. **A622** (2010) 231.
- [24] T. R. Saito, S. Bianchin, O. Borodina, J. Hoffmann *et al.*, Int. J. Mod. Phys. **E19** (2010) 2656.
- [25] GSI Scientific report, PHN-NQM-FOPI-03.
- [26] T. Gaitanos, H. Lenske, U. Mosel, Phys. Lett. **B675** (2009) 297.
- [27] M. Danysz *et al.*, Nucl. Phys. **49** (1963) 121.
- [28] D.J. Prowse, Phys. Rev. Lett. **17** (1966) 782.
- [29] K. Nakazawa for KEK-E176, E373 and J-PARC E07 collaborators, Nucl. Phys. **A835** (2010) 207.
- [30] A. Sanchez Lorente, P. Achenbach, J. Pochodzalla, S. Sanchez Majos, To appear in: Nuclear Science Symposium Conference, 2008 (NSS '08), p. 1655, doi:10.1109/NSSMIC.2008.4774720, in press.
- [31] J. Pochodzalla, Nucl. Instrum. Methods **B214** (2004) 149.
- [32] PANDA Collaboration, Technical Progress Report for PANDA: Strong Interaction Studies with Antiprotons, 2005.
- [33] F. Ferro, M. Agnello, F. Iazzi, K. Szymanska, Nucl. Phys. **A789** (2007) 209.
- [34] K. Nakamura *et al.* (Particle Data Group), J. Phys. **G37** (2010) 075021.

- [35] T.R. Saito (HypHI Collaboration), private communication.
- [36] O. Buss, T. Gaitanos, K. Gallmeister, H. van Hees, M. Kaskulov, O. Lalakulich, A. B. Larionov, T. Leitner *et al.*, [arXiv:1106.1344 [hep-ph]].
- [37] A.S. Botvina *et al.*, Nucl. Phys. **A475** (1987) 663;
J.P. Bondorf *et al.*, Phys. Rept. **257** (1995) 133.
- [38] L.P. Kadanoff, G. Baym, *Quantum Statistical Mechanics* (Benjamin, N.Y. 1962).
- [39] W. Botermans, R. Malfliet, Phys. Rept. **198** (1990) 115.
- [40] B. D. Serot, J. D. Walecka, Int. J. Mod. Phys. **E6** (1997) 515.
- [41] G. A. Lalazissis, S. Karatzikos, R. Fossion, D. Pena Arteaga, A. V. Afanasjev, P. Ring, Phys. Lett. **B671** (2009) 36.
- [42] S. Teis, W. Cassing, T. Maruyama, U. Mosel, Phys. Rev. **C50** (1994) 388.
- [43] T. Gaitanos, M. Kaskulov, U. Mosel, Nucl. Phys. **A828** (2009) 9, [arXiv:0904.1130 [nucl-th]].
- [44] T. Gaitanos, M. Kaskulov, H. Lenske, Phys. Lett. **B703** (2011) 193, [arXiv:1105.4450 [nucl-th]].
- [45] T. Gaitanos, M. Kaskulov, [arXiv:1109.4837 [nucl-th]].
- [46] A. B. Larionov, I. A. Pshenichnov, I. N. Mishustin, W. Greiner, Phys. Rev. **C80** (2009) 021601.
- [47] A. B. Larionov, T. Gaitanos, U. Mosel, [arXiv:1107.2326 [nucl-th]].
- [48] E.S. Golubeva *et al.*, Nucl. Phys. **A537** (1992) 393;
I.A. Pshenichnov, doctoral thesis, INR, Moskow, 1998.
- [49] C. B. Dover, T. Gutsche, M. Maruyama, A. Faessler, Prog. Part. Nucl. Phys. **29** (1992) 87.
- [50] A. Reuber, K. Holinde, J. Speth, Nucl. Phys. **570** (1994) 543.
- [51] J. Haidenbauer, U. -G. Meissner, Phys. Rev. **C72** (2005) 044005.
- [52] J.J. de Swart, T.A. Rijken, P.M. Maessen, R.G.E. Timmermans, Nuovo Cimento, **102** (1989) 203.
- [53] Landolt-Börnstein, New Series I/12b.
- [54] T. A. Rijken, Y. Yamamoto, [nucl-th/0608074].
- [55] T. Gaitanos, H. Lenske, U. Mosel, Phys. Lett. **B663** (2008) 197, [arXiv:0712.3292 [nucl-th]].
- [56] C.Y. Wong, Phys. Rev. **C25** (1982) 1460;
C. Gregoire, B. Remaud, F. Sebillé, L. Vinet, Y. Raffray, Nucl. Phys. **465** (1987) 317.

- [57] T. GaiTanos, A. B. Larionov, H. Lenske, U. Mosel, Phys. Rev. **C81** (2010) 054316, [arXiv:1003.4863 [nucl-th]].
- [58] B. Lott, F. Goldenbaum, A. Böhm, W. Bohne *et al.*, Phys. Rev. **C63** (2001) 034616.
- [59] M.R. Clover, R.M. DeVries, N.J. DiGiacomo, Y. Yariv, Phys. Rev. **C26** (1982) 2138.
- [60] V. Flaminio, I.F. Graf, J.D. Hansen, W.G. Moorhead, D.R.O. Morrison, CERN-HERA 79-03 (Geneva, 1979, <http://cdsweb.cern.ch/record/101338/files/cm-p00048064.pdf>)
- [61] V. Flaminio, W.G. Moorhead, D.R.O. Morrison, N. Rivoire, CERN-HERA 83-02 (Geneva, 1983, <http://cdsweb.cern.ch/record/101337/files/cm-p00048060.pdf>).